Longitudinal Studies of Angiogenesis in Hormone-Dependent Shionogi Tumors[1,2]

Trevor P. Wade* and Piotr Kozlowski[†,‡,§,¶]

*Department of Physics and Astronomy, University of British Columbia, Vancouver, BC, Canada; [†]The Prostate Center at Vancouver General Hospital, Vancouver, BC, Canada; [‡]Department of Urologic Sciences, University of British Columbia, Vancouver, BC, Canada; [§]Department of Radiology, University of British Columbia, Vancouver, BC, Canada; [¶]UBC MRI Research Center, University of British Columbia, Vancouver, BC, Canada

Abstract

Vessel size imaging was used to assess changes in the average vessel size of Shionogi tumors throughout the tumor growth cycle. Changes in R_2 and R_2^* relaxivities caused by the injection of a superparamagnetic contrast agent (ferumoxtran-10) were measured using a 2.35-T animal magnetic resonance imaging system, and average vessel size index (VSI) was calculated for each stage of tumor progression: growth, regression, and relapse. Statistical analysis using Spearman rank correlation test showed no dependence between vessel size and tumor volume at any stage of the tumor growth cycle. Paired Student's t test was used to assess the statistical significance of the differences in average vessel size for the three stages of the tumor growth cycle. The average VSI for regressing tumors (15.1 ± 6.6 μm) was significantly lower than that for growing tumors (35.2 ± 25.5 μm; $P < .01$). Relapsing tumors also had an average VSI (45.4 ± 41.8 μm) higher than that of regressing tumors, although the difference was not statistically significant ($P = .067$). This study shows that VSI imaging is a viable method for the noninvasive monitoring of angiogenesis during the progression of a Shionogi tumor from androgen dependence to androgen independence.

Neoplasia (2007) **9,** 563–568

Keywords: Magnetic resonance imaging, vessel size imaging, angiogenesis, hormone-dependent tumors, tumor microenvironment.

Introduction

Among American men, prostate cancer is currently the most common and second most deadly form of cancer (after lung cancer) [1]. Early detection greatly increases the efficacy of possible treatment regimens: surgery to remove the tumor or radiation therapy (either external therapy or brachytherapy). Once the tumor has metastasized, the likelihood of survival drops drastically, and the only effective form of systemic therapy is androgen withdrawal [2]. Prostate cancer is one of many solid tumors that are hormone-dependent. Several studies in animal models of hormone-dependent tumors suggest a strong correlation between hormonal status and tumor microenvironment, including blood supply [3].

Tumor microenvironment is an essential factor in the biology and physiology of solid tumors, and it contributes to diagnostic features and therapeutic response. Particularly important is tumor blood supply, as many physiological parameters, such as tissue oxygenation, metabolism, pH, and nutrient supply, directly or indirectly depend on it [4].

Not only does vasculature supply the tumor with nutrients necessary for growth, but, more importantly, there are an increasing number of studies showing that the very nature of tumor microvessels is strongly linked to the formation of metastases. Weidner et al. [5] found that, in prostate cancer, microvessel density correlates with both Gleason score and metastasis. Angiogenic tumor cells promote new capillaries, which have a leaky basement membrane. This allows tumor cells easier access to the bloodstream and thus increases the likelihood of metastasis. Moreover, cells forming the new tumor are more likely to be angiogenic.

Thus, the growth of tumor microvasculature appears to be critical to primary tumor growth and is a key factor in the formation of metastases and, as a result, is linked to survival [6]. Vascular endothelial growth factor (VEGF) appears to be the primary signal for tumor vascularization. It is expressed at low levels in normal tissues and appears to be linked to tumor growth and angiogenesis in prostate tumors. It is expressed at high levels during tumor growth, but androgen ablation leads to a decrease in VEGF expression by tumor cells, resulting in apoptosis of endothelial and tumor cells, leading to normalization of tumor vasculature. With relapse, though, VEGF production is increased again [7].

For this reason, it has been proposed that a combined hormone and antiangiogenic regimen could potentially be very effective at treating prostate cancer [5,7–9]. Normalizing the tumor vasculature through an anti-VEGF has the added benefit that it will improve the delivery and effectiveness of conventional cytotoxic and molecularly targeted therapies [8].

Measuring microvasculature to monitor the effectiveness of these novel therapies is not easy. Jain et al. [7] and Borgstrom et al. [6] used dorsal skinfold chambers in mice, and Weidner et al. [5] used biopsy tissues to assess the tumor microvasculature. Both of these techniques are invasive and allow only part of the tumor to be observed. Tropres et al. [10] proposed a novel contrast-enhanced technique for characterizing the tumor vasculature. By measuring the increase in transverse relaxation rates ΔR_2 and ΔR_2^* caused by the injection of an ultrasmall superparamagnetic iron oxide (USPIO) contrast agent, it is possible to measure a weighted average of blood vessel radii, known as the vessel size index (VSI) [10].

The work of Tropres et al. [10,11] focused on brain tumors and made the assumption that the blood–brain barrier remained intact and that the contrast agent did not leak into tissues during scanning. In this study, we evaluated the feasibility of using VSI techniques to measure long-term changes in the blood supply of subcutaneous tumors and to assess the correlation between angiogenesis and a tumor's hormonal status in the Shionogi model of prostate cancer. To our knowledge, this is the first application of the VSI technique to investigate subcutaneous tumors in a longitudinal study.

Materials and Methods

Animal Preparation

All animal experimental procedures were carried out in compliance with the guidelines of the Canadian Council for Animal Care and were approved by the institutional Animal Care Committee. The Toronto subline of transplantable SC-115 AD mouse mammary carcinoma [12] was used in all experiments. Seventeen male DD/S mice were inoculated subcutaneously with approximately 5×10^6 Shionogi cells on their lower back.

In preparation for imaging, the mice were anaesthetized with 4% isoflurane in air and then maintained at 1.5%. The mice were placed on their back on an imaging bed with the tumor centered in the coil. Body temperature was maintained at 35°C to 37°C using a hot water heating pad and was monitored with a rectal probe. Remote injection of 200 μmol Fe/kg contrast agent (ferumoxtran-10; Advanced Magnetics, Cambridge, MA), followed by an approximately 0.05-ml saline flush, was accomplished using a 27-gauge 1/2-in.-long needle inserted into the tail vein and attached to a 0.38-mm-inner-diameter polyethylene tubing.

Of 17 mice used in this study, 2 were euthanized precastration due to ulcerating tumors, 2 died from complications from castration, and 1 died in the magnet during imaging for the second regression time point. Of the 12 remaining mice, only 6 had relapsed androgen-independent tumors 15 weeks following inoculation. Two VSI measurements were attempted at least 48 hours apart for each stage of tumor progression in each mouse.

Magnetic Resonance Imaging (MRI) Experiments

All MRI experiments were performed on a 2.35-T, 40-cm-bore magnet (Bruker, Ettlingen, Germany) equipped with an SMIS (SMIS, Surrey, UK) console using a 2.5-cm-diameter three-turn solenoid coil. Imaging was performed in the transverse plane on a 2-mm-thick slice through the center of the tumor using a 128×128 matrix and a field of view of 40 mm. For ΔR_2 measurements, a spin-echo sequence with a repetition time (T_R) of 2500 milliseconds and an echo time (T_E) of 60 milliseconds was used; for ΔR_2^* measurements, a gradient-echo sequence with T_R/T_E = 2500/10 milliseconds was used. Apparent diffusion coefficient (ADC) was measured using a diffusion-weighted spin-echo sequence with T_R/T_E = 2500/60 milliseconds and a gradient factor b of 1000 sec/mm^2 (distance between diffusion-sensitizing gradients Δ = 35 milliseconds; duration of each diffusion-sensitizing gradient δ = 15 milliseconds; amplitude G = 45.5 mT/m). A multislice proton density-weighted (T_R/T_E = 2500/10 milliseconds) sequence was used for tumor volume measurements.

Blood Susceptibility Measurements

For susceptibility measurements, five mice were injected with 200 μmol/kg contrast agent, as described previously. After allowing the agent to perfuse for 10 minutes, blood was drawn out of the heart. Blood from the mice was mixed together and with heparin to prevent clotting. A sample was then taken for analysis on an Instrumentation Laboratory Micro 13 pH/Blood Gas analyzer for pO$_2$, pCO$_2$, and blood pH measurements and for centrifugation for hematocrit.

The susceptibility of blood with contrast agent was measured using a nuclear magnetic resonance spectroscopy method [10]. Two 1.1-mm-inner-diameter heparinized glass tubes filled with distilled water were placed in a 1.5-ml plastic vial perpendicular to each other. The drawn blood was placed in the vial and then the vial in the magnet, with one of water-filled capillaries aligned parallel to the magnetic field B_0 and with the other perpendicular to it. Susceptibility was calculated from the difference in the resonant frequencies of water in the two capillaries [10]. The susceptibility of blood without contrast agent was calculated from measured hematocrit and oxygen saturation hemoglobin values using the formula described by Tropres et al. [10]. The susceptibility of oxygenated and deoxygenated red blood cells was assumed to be $0.33 \pm 0.09 \times 10^{-6}$ and $1.97 \pm 0.09 \times 10^{-7}$, respectively [13].

Data Processing and Analysis

All MRI data were processed offline with a software package developed in-house using MATLAB (The MathWorks, Inc., Natick, MA).

Tumor VSI was calculated by measuring the total signal from a region of interest (ROI) encompassing the entire
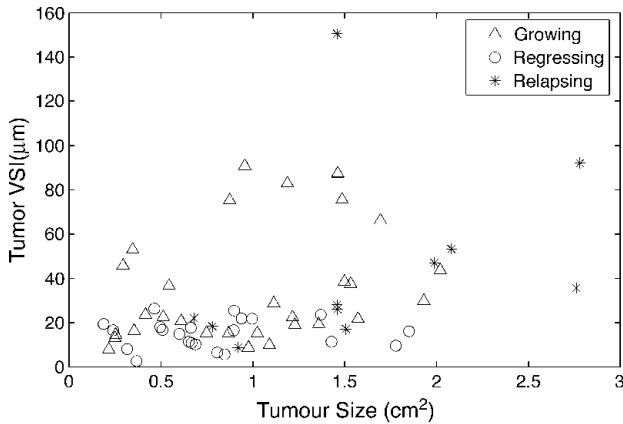
Figure 1. *VSI appears to be independent of tumor size. Overall Spearman rank correlation coefficient r_s = 0.386 (P = .003).*

tumor in the slice and using that to calculate the ΔR_2, ΔR_2^*, and ADC values of the tumor [10]. Tumor volumes were calculated from multislice proton density-weighted spin-echo images. The border of the tumor was outlined manually on each of the images, and tumor volume was calculated by taking the sum of the areas in each slice multiplied by slice thickness.

The animals were divided into three experimental groups corresponding to the three stages of the tumor progression cycle: growth, regression, and relapse. Spearman rank–order correlation coefficient was used to test for any correlation between VSI and tumor size. Paired Student's *t* test was used to assess for differences in VSI throughout the tumor progression cycle. In addition, Kolmogorov-Smirnov test was used to compare VSI distributions between the three experimental groups.

Results

The increase in blood susceptibility caused by the contrast agent $\Delta\chi$ was measured to be 6.37 ± 0.15 ppm.

Statistical analysis of all tumors using Spearman rank correlation test showed no dependence between vessel size and tumor volume at any stage of the tumor growth cycle (overall Spearman rank correlation coefficient r_s = 0.386, P = .003; Figure 1).

Only six tumors successfully progressed to an androgen-independent state. Figure 2 shows axial cross-sections through the center of a representative tumor acquired at different stages of the tumor growth cycle. Calculated VSI maps are shown in the bottom row. The average VSI values from an ROI encompassing the entire tumor were 44, 6, and 92 μm for the growing, regressing, and relapsing stages, respectively.

The average VSI for each stage of tumor progression was calculated using all measurements made on mice in that stage and is shown in Table 1. In the 13 mice whose tumors regressed, all but 2 saw their mean VSI decrease postcastration; of the 6 mice that progressed to an androgen-independent state, all but 1 experienced a subsequent increase in tumor VSI (Figure 3). The longitudinal nature of this study lends itself well to an analysis that takes into consideration the dependent nature of measurements; hence, paired Student's *t* test was used to test the significance of changes in tumor VSI. With a *t* statistic of 3.205 (P = .0076), there is strong evidence to support a decrease in vessel size postcastration in regressing tumors. The *t* statistics for the difference between regressing and relapsing tumors and between growing and relapsing tumors are −2.417 (P = .067) and −0.215 (P = .838), respectively.

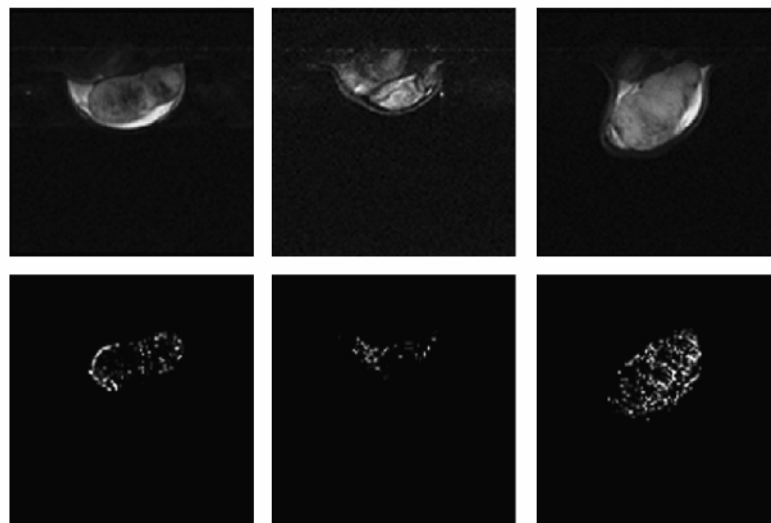Figure 4 shows a histogram of pixel VSI for all tumors grouped into growing, regressing, and relapsing tumors.

Figure 2. *Axial cross-sections (top row) and VSI maps (bottom row) for a representative tumor at the growing (left column), regressing (middle column), and relapsing (right column) stages of the tumor growth cycle. The average VSI value was 44 μm for the growing tumor, 6 μm for the regressing tumor, and 92 μm for the relapsing tumor.*

Table 1. Average Tumor VSI Measurements in Each Stage of Shionogi Tumor Progression.

Tumor Type	VSI (μm)	SD	n Measurements (n Mice)
Growing	35.2	25.5	30 (17)
Regressing	15.1	6.56	22 (13)
Relapsing	45.4	41.8	11 (6)

Regressing tumors had the largest number of small vessels (VSI < 15 μm), whereas relapsing tumors had the largest number of medium and large vessels (VSI > 30 μm). A Kolmogorov-Smirnov test showed statistically significant differences in VSI distributions between the three experimental groups (Table 2).

Figure 4. *Histogram of pixel VSI for all tumors grouped into growing, regressing, and relapsing tumors.*

Discussion

In this study, we examined changes in average vessel size throughout the tumor growth cycle in the Shionogi model of prostate cancer. Our results show that the VSI, which is a measure of vessel radius, decreases significantly following androgen ablation. The most likely reason for this decrease is the reduction in the levels of VEGF following androgen ablation. Shweiki et al. [14] showed that regressing tumor vessels experience a significant reduction in their diameters following VEGF neutralization with a blocking antibody. Because androgen ablation results in a significant decrease in VEGF levels in Shionogi tumors [7], this decrease will subsequently trigger a concomitant decrease in vessel sizes.

Relapsing tumors showed increased vessel sizes, although the difference in average VSI between regressing and relapsing tumors failed to reach statistical significance ($P = .067$). This increase in VSI represents the second wave of angiogenesis, which was also reported by Jain et al. [7]. It is interesting to note that vessels in relapsing androgen-independent tumors were generally larger than vessels in the original growing androgen-dependent tumors, as evidenced by a comparison of vessel size distribution in all three groups of tumors (Figure 4). This increased number of medium and larger vessels (VSI > 30 μm) in relapsing tumors may be
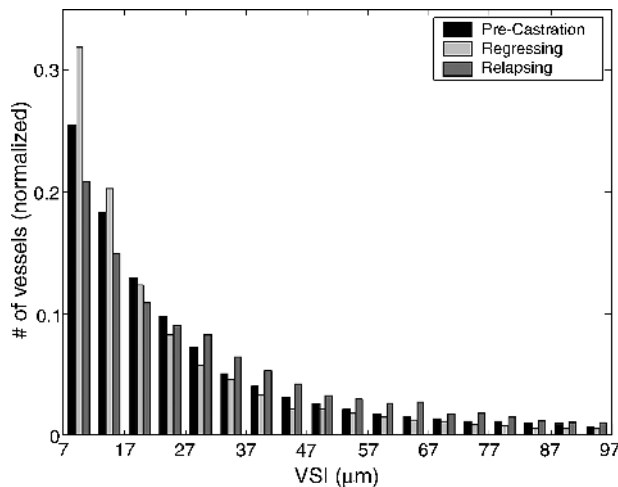
related to slower tumor growth in this phase of the growth cycle, which allows more significant vessels to form. This is also supported by our previous study, which showed significantly less heterogeneity in the perfusion pattern and higher perfusion levels in androgen-independent *versus* androgen-dependent Shionogi tumors [3]. The increased vessel sizes in androgen-independent tumors may also reflect a more aggressive phenotype of these tumors. It has been shown that the size of vessels within a tumor varies with its aggresiveness [15]. It is also known that androgen-independent prostate tumors are more aggressive and are more likely to metastasize. Thus, vessel size imaging may potentially provide a noninvasive way of assessing tumor aggressiveness and propensity for metastasis, although more thorough studies are required to test this hypothesis.

The vessel size imaging technique used in this study relies on the contrast agent remaining in the vasculature following injection for the duration of MRI measurements. The permeability of tumor vessels is typically much higher than that of vessels in normal tissues; thus, low-molecular-weight agents typically leak out of the vasculature within minutes of injection. The contrast agent used in this study is
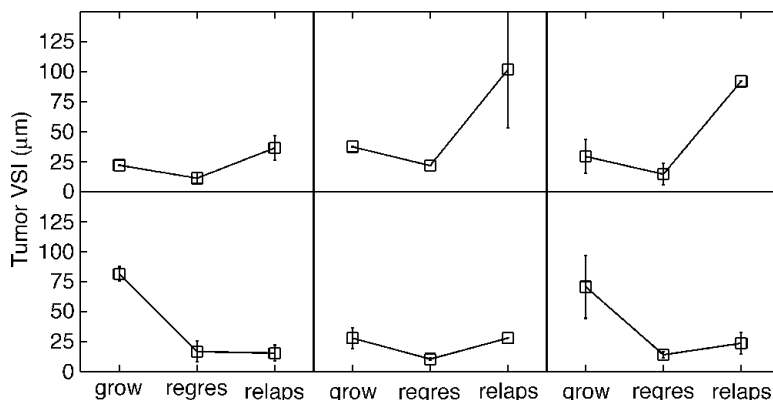
Figure 3. *Tumor VSI trends of six mice that progressed to an androgen-independent state. Error bars indicate the range of values for each average, where available.*

Table 2. Kolmogorov-Smirnov *d* Statistic for the Difference between Distributions and Associated Significance Values.

	d	*P*
Growing *versus* regressing tumors	0.087	⩽ .01
Growing *versus* relapsing tumors	0.109	⩽ .01
Regressing *versus* relapsing tumors	0.182	⩽ .01

part of a class of agents known as USPIO particles and has been designed as a blood pool contrast agent. It consists of an iron oxide core 4 to 6 nm in diameter coated in a dextran shell (8–12 nm thick) to form a relatively inert particle. The thick dextran layer reduces the reaction of the particle with plasma proteins and reduces the rate at which particles are eliminated by phagocytosis [16]. This yields a particle contrast agent with a relatively long half life of 4.5 hours in rat blood plasma [10].

The validity of VSI measurements is limited by specific assumptions in formulating the theory behind this technique. In the lower limit, static dephasing and slow diffusion approximations limit measurements of VSI to values of > 7 μm [10]. The upper limit of validity for VSI measurements is based on the need for sufficient averaging over the voxel for the analytic spin-echo equation to be valid, thus setting an upper limit of 50 μm based on an ROI encompassing the tumor on a 2-mm slice [17]. These limitations are likely the reason for the differences between our results and those of Jain et al. [7], who used dorsal skinfold chambers and optical microscopy to assess changes in vessel diameter in Shionogi tumors following androgen ablation. We measured the mean VSI for growing tumors to be 35.2 μm, whereas Jain et al. reported a mean vessel radius of 19.2 μm immediately before castration. In addition, Jain et al. saw the mean vessel radius drop to 13.3 μm at 2 to 3 days postcastration and further drop to 4.7 μm at 2 weeks postcastration. We measured the average VSI for regressing tumors to be 15.1 μm, with the average time of measurement at 6 days postcastration. Overestimation of vessel sizes is likely due to the fact that the lower limit of 7 μm used in calculating the mean VSI cuts off a large fraction of the vessels and that the imaging technique leads to an underestimation of ΔR_2. This is consistent with previous reports of overestimation of vessel diameters using the vessel size imaging technique [10,18].

In addition to tumor VSI measurements, it is also possible to construct a VSI map of the tumor by calculating the VSI for each pixel (Figure 2). Although the statistical limits described above are not satisfied by each pixel, the map gives valuable information on the distribution of blood vessels [11] and can be used to correlate VSI results with histology [19]. In the current study, we did not carry out a quantitative correlation between VSI maps and the corresponding histologic slides; however, a qualitative comparison between VSI maps and vessel distributions obtained with Hoechst dye 33342 (Sigma-Aldrich, St. Louis, MO) staining (data not shown) demonstrated generally good agreement. For larger tumors, where statistical limits of VSI measurements are fulfilled, generating quantitative VSI maps could provide a very useful way to monitor the effectiveness of combined antiangiogenic therapies and could

possibly offer a noninvasive screening and grading technique for prostate and other cancers.

Although a number of studies on the application of blood pool contrast agents to investigate the tumor vasculature have been reported before, vessel size imaging is a relatively new technique [19–24]. A majority of these studies have been carried out on brain tumors and have focused on testing the limitations of this technique [11,25,26] and on correlating MRI results with histology [11,19,20,22]. To our knowledge, the current study is the first study where vessel size imaging has been applied to examine longitudinal changes in VSI within the same tumors. The noninvasive character of this technology is particularly suitable for longitudinal investigation; considering that solid tumors are typically heterogeneous, studying the same tumors over time will more likely provide statistically significant results, which was the case in our study.

Vessel size imaging seems ideal to study *in vivo* the function and morphology of the tumor vasculature, which plays a critical role in tumor growth; its propensity to metastasize; and its potential response to chemotherapy and radiotherapy [27]. There has been recent increased interest in antiangiogenic antivascular cancer therapies. Because many of these therapies do not result in a significant growth delay in tumor xenografts [28], vessel size imaging can provide a noninvasive way of testing the efficacy of such therapies. Recently, Kiselev et al. [18] applied the vessel size imaging technique in brain tumor patients. They used a low-molecular-weight contrast agent (Gd-DTPA) rather than a blood pool contrast agent used commonly in VSI measurements. To avoid problems with the contrast agent leaking out of the vasculature, a very fast imaging technique (echo planar imaging) had to be used to generate ΔR_2 and $\Delta R_2{}^*$ maps during the first pass of the bolus of the contrast agent. As a result of the required very high temporal resolution, spatial resolution in MRI images had to be sacrificed. Nevertheless, they were able to generate quantitative measures of vessel sizes in the tumors and normal brain tissues, demonstrating that this technique can be used to study human tumors. Considering the great research effort in developing new MRI contrast agents over the last decade, large-molecular-weight blood pool contrast agents will likely be approved for human use soon. This will allow application of the vessel size imaging technique in humans.

Conclusion

Vessel size imaging has proven to be a viable method of monitoring angiogenesis during the progression of a Shionogi tumor from androgen dependence to androgen independence. It appears to work well for subcutaneous tumors and has proven capable of distinguishing differences in the vasculature between the different stages of tumor progression.

Acknowledgements

References

[1] Jemal A, Tiwari RC, Murray T, Ghafoor A, Samuels A, Ward E, Feuer EJ, and Thun MJ (2004). Cancer statistics, 2004. *CA Cancer J Clin* **54**, 8–29.

[2] Miayake H, Tolcher A, and Gleave ME (2000). Chemosensitization and delayed androgen-independent recurrence of prostate cancer with the use of antisense Bcl-2 oligodeoxynucleotides. *J Natl Cancer Inst* **92**, 34–41.

[3] Kozlowski P, Wong J, and Goldenberg SL (2005). Serial tumour blood-flow measurements in androgen-dependent and -independent Shionogi tumour models. *BJU Int* **95**, 644–649.

[4] Vaupel P, Kallinowski F, and Okunieff P (1989). Blood flow, oxygen and nutrient supply, and metabolic microenvironment of human tumors: a review. *Cancer Res* **49**, 6449–6465.

[5] Weidner N, Carroll PR, Flax J, Blumenfeld W, and Folkman J (1993). Tumor angiogenesis correlates with metastasis in invasive prostate carcinoma. *Am J Pathol* **143**, 401–409.

[6] Borgstrom P, Bourdon MA, Hillan KJ, Sriramarao P, and Ferrara N (1998). Neutralizing anti-vascular endothelial growth factor antibody completely inhibits angiogenesis and growth of human prostate carcinoma micro tumors *in vivo*. *Prostate* **35**, 1–10.

[7] Jain RK, Safabakhsh N, Sckell A, Chen Y, Jiang P, Benjamin L, Yuan F, and Keshet E (1998). Endothelial cell death, angiogenesis, and microvascular function after castration in an androgen-dependent tumor: role of vascular endothelial growth factor. *Proc Natl Acad Sci USA* **95**, 10820–10825.

[8] Jain RK (2001). Normalizing tumor vasculature with anti-angiogenic therapy: a new paradigm for combination therapy. *Nat Med* **7**, 987–989.

[9] Melnyk O, Zimmerman M, Kim KJ, and Shuman M (1999). Neutralizing anti-vascular endothelial growth factor antibody inhibits further growth of established prostate cancer and metastases in a pre-clinical model. *J Urol* **161**, 960–963.

[10] Tropres I, Grimault S, Vaeth A, Grillon E, Julien C, Payen JF, Lamalle L, and Decorps M (2001). Vessel size imaging. *Magn Reson Med* **45**, 397–408.

[11] Tropres I, Lamalle L, Peoc'h M, Farion R, Usson Y, Decorps M, and Remy C (2004). *In vivo* assessment of tumoral angiogenesis. *Magn Reson Med* **51**, 533–541.

[12] Rennie PS, Bruchovsky N, Buttyan R, Benson M, and Cheng H (1988). Gene expression during the early phases of regression of the androgen-dependent Shionogi mouse mammary carcinoma. *Cancer Res* **48**, 6309–6312.

[13] Weisskoff RM and Kiihne S (1992). MRI susceptometry: image-based measurement of absolute susceptibility of MR contrast agents and human blood. *Magn Reson Med* **24**, 375–383.

[14] Shweiki D, Itin A, Soffer D, and Keshet E (1992). Vascular endothelial growth factor induced by hypoxia may mediate hypoxia-initiated angiogenesis. *Nature* **359**, 843–845.

[15] Papadimitriou JM and Woods AE (1975). Structural and functional characteristics of the microcirculation in neoplasms. *J Pathol* **116**, 65–72.

[16] Jung CW and Jacobs P (1995). Physical and chemical properties of superparamagnetic iron oxide MR contrast agents: ferumoxides, ferumoxtran, ferumoxsil. *Magn Reson Imaging* **13**, 661–674.

[17] Kiselev VG and Posse S (1999). Analytical model of susceptibility-induced MR signal dephasing: effect of diffusion in a microvascular network. *Magn Reson Med* **41**, 499–509.

[18] Kiselev VG, Strecker R, Ziyeh S, Speck O, and Hennig J (2005). Vessel size imaging in humans. *Magn Reson Med* **53**, 553–563.

[19] Robinson SP, Rijken PF, Howe FA, McSheehy PM, van der Sanden BP, Heerschap A, Stubbs M, van der Kogel AJ, and Griffiths JR (2003). Tumor vascular architecture and function evaluated by non-invasive susceptibility MRI methods and immunohistochemistry. *J Magn Reson Imaging* **17**, 445–454.

[20] Dennie J, Mandeville JB, Boxerman JL, Packard SD, Rosen BR, and Weisskoff RM (1998). NMR imaging of changes in vascular morphology due to tumor angiogenesis. *Magn Reson Med* **40**, 793–799.

[21] Le Duc G, Peoc'h M, Remy C, Charpy O, Muller RN, Le Bas JF, and Decorps M (1999). Use of T(2)-weighted susceptibility contrast MRI for mapping the blood volume in the glioma-bearing rat brain. *Magn Reson Med* **42**, 754–761.

[22] Kostourou V, Robinson SP, Whitley GS, and Griffiths JR (2003). Effects of overexpression of dimethylarginine dimethylaminohydrolase on tumor angiogenesis assessed by susceptibility magnetic resonance imaging. *Cancer Res* **63**, 4960–4966.

[23] Reichardt W, Hu-Lowe D, Torres D, Weissleder R, and Bogdanov A Jr (2005). Imaging of VEGF receptor kinase inhibitor-induced antiangiogenic effects in drug-resistant human adenocarcinoma model. *Neoplasia* **7**, 847–853.

[24] Bradley DP, Tessier JJ, Ashton SE, Waterton JC, Wilson Z, Worthington PL, and Ryan AJ (2007). Correlation of MRI biomarkers with tumor necrosis in hras5 tumor xenograft in athymic rats. *Neoplasia* **9**, 382–391.

[25] Tropres I, Grimault S, Vaeth A, Grillon E, Julien C, Payen JF, Lamalle L, and Decorps M (2001). Vessel size imaging. *Magn Reson Med* **45**, 397–408.

[26] Tropres I, Lamalle L, Farion R, Segebarth C, and Remy C (2004). Vessel size imaging using low intravascular contrast agent concentrations. *MAGMA* **17**, 313–316.

[27] Carmeliet P and Jain RK (2000). Angiogenesis in cancer and other diseases. *Nature* **407**, 249–257.

[28] Cristofanilli M, Charnsangavej C, and Hortobagyi GN (2002). Angiogenesis modulation in cancer research: novel clinical approaches. *Nat Rev Drug Discov* **1**, 415–426.